# Anomalocaridid trunk limb homology revealed by a giant filter-feeder with paired flaps

Peter Van Roy[1, 2], Allison C. Daley[3, 4] & Derek E. G. Briggs[1, 5]

[1] Department of Geology and Geophysics, Yale University, PO Box 208109, New Haven, Connecticut 06520, USA. [2]Research Unit Palaeontology, Department of Geology and Soil Science, Ghent University, Krijgslaan 281/S8, B-9000 Ghent, Belgium. [3]Department of Zoology, University of Oxford, The Tinbergen Building, South Parks Road, Oxford OX1 3PS, UK. [4]Oxford University Museum of Natural History, Parks Road, Oxford OX1 3PW, UK. [5]Yale Peabody Museum of Natural History, Yale University, New Haven, Connecticut 06520, USA.

**Palaeozoic exceptionally preserved fossils provide crucial insights into arthropod evolution, with recent discoveries bringing phylogeny and character homology into sharp focus [1, 2, 3, 4]. Integral to such studies are anomalocaridids, a clade of stem arthropods whose remarkable morphology illuminates early arthropod relationships[5, 6] and Cambrian ecology[7, 8, 9]. Although recent work focused on the anomalocaridid head[6-10], the nature of their trunk has been debated widely[5, 11-18]. Here we describe new anomalocaridid[17] specimens from the Early Ordovician Fezouata Biota of Morocco[19], which not only show well-preserved head appendages providing key ecological data, but also elucidate the nature of anomalocaridid trunk flaps, resolving their homology with arthropod trunk limbs. The new material shows that each trunk segment bears a separate dorsal and ventral pair of flaps, with a series of setal blades attached at the base of the dorsal flaps. Comparisons with other stem lineage arthropods[16, 20-22] indicate that anomalocaridid ventral flaps**

**are homologous with lobopodous walking limbs and the endopod of the euarthropod biramous limb, while the dorsal flaps and associated setal blades are homologous with the flaps of gilled lobopodians (e.g. *Kerygmachela kierkegaardi*, *Pambdelurion whittingtoni*) and exites of the "Cambrian biramous limb"[23]. This evidence shows anomalocaridids occupy a stage before the fusion of exite and endopod into the "Cambrian biramous limb"[5, 16, 23], confirming their basal placement in the euarthropod stem[4, 5, 6], rather than in the arthropod crown[24] or with cycloneuralian worms[14]. Unlike other anomalocaridids, the Fezouata taxon combines head appendages convergently[9] adapted for filter-feeding with an unprecedented body length exceeding 2 m, indicating a new direction in the feeding ecology of the clade. The evolution of giant filter-feeding anomalocaridids may reflect the establishment of highly developed planktic ecosystems during the Great Ordovician Biodiversification Event[25].**

Phylum Arthropoda von Siebold, 1848

Order Radiodonta Collins, 1996

Family Hurdiidae Vinther, Stein, Longrich & Harper, 2014

***Aegirocassis benmoulae*** gen. et sp. nov.

**Life Science Identifier (LSID).** urn:lsid:zoobank.org:act:35C7BB1E-C902-4F7B-9A4B-899005D7B6AE

**Etymology.** *Ægir* (a giant in Norse mythology and god of the sea) + *cassis* (Latin, helmet): referring to the huge size and elaborate cephalic shield; and in recognition of

Mohamed “Ou Said” Ben Moula, who discovered the Fezouata Biota and the specimens described here. Gender feminine.

**Holotype.** Holotype Yale Peabody Museum YPM 237172 (Fig. 1, Extended Data Figs 1, 2, Supplementary Video).

**Other material.** Paratypes YPM 227556 (Extended Data Fig. 3c, d), YPM 525437 (Extended Data Fig. 4, Supplementary Video), YPM 527123 (Extended Data Fig. 5a-c), YPM 527125 (Fig. 2a-b, Extended Data Fig. 6a), YPM 226437, YPM 222227 (Fig. 2c, Extended Data Fig. 7a-c). Other notable specimens YPM 226438, YPM 226439, YPM 523423-523427 (Extended Data Figs 3e-h, 5g, 7d, e), YPM 523428 (Extended Data Fig. 5f), YPM 516785 (Extended Data Fig. 3a, b), YPM 523810 (Extended Data Fig. 5e), YPM 525217 (Extended Data Fig. 6b-d), YPM 516791 (Extended Data Fig. 8a-c), YPM 227934 (Extended Data Fig. 8e), YPM 516792 (Extended Data Fig. 8f) and YPM 527124 (Extended Data Fig. 5d), and setal blades associated with YPM 527123 (Extended Data Fig. 8d). Fragmentary material of three other articulated individuals, four slabs with disarticulated material belonging to at least 10 individuals, 15 isolated carapace elements, 14 sets of partial ventral spines and 11 isolated bands of setal blades.

**Locality and horizon.** Lower Fezouata Formation, latest Tremadocian, *Araneograptus murrayi* Biozone. All three-dimensional specimens were collected from two sites on the eastern flank of Jbel Tigzigzaouine, facing Oued Ezegzaou. Specimens of carapaces, setal blades and ventral spines of the frontal appendages occur at numerous sites throughout the Lower Fezouata Formation to the north of Zagora, often in abundance. Detailed locality information is curated with the specimens.

**Diagnosis for genus and species.** Anomalocaridid with tripartite frontal carapace having a central element at least as long as trunk, with an axial carina, pointed tip, rounded posterior margin and narrow downturned postero-ventral triangular extensions tapering towards rear and overlapping the lateral carapace elements dorsally. Lateral carapace elements oval, with rounded antero-dorsal expansion and longitudinal carina just below midline. Multisegmented anterior appendages consisting of seven podomeres. First podomere longest, with one shorter, comb-like ventral spine proximally. Succeeding five podomeres each with a single elongate, inward-angled ventral spine with stout setae bearing a double row of fine spinules set in a V on their dorsal margin. Terminal podomere stout, with pointed tip. Flat, broad trunk of 11 segments attaining maximum width at third segment and tapering to a blunt tip. Two pairs of non-overlapping flaps per segment: dorsal flaps pointed with recurving anterior and posterior margins, width ca 1× length of their attachment; ventral flaps narrow, triangular, width ca 1.5× length of their attachment. Continuous band of dorsal setal blades attached to base of each pair of dorsal flaps, traversing the trunk.

A detailed description and interpretation of the material, including the filter feeding frontal appendages, is provided in the Supplementary Text. The holotype YPM 237172 is an almost complete three-dimensionally preserved individual in slightly oblique dorsal view (Fig. 1, Extended Data Fig. 1, Supplementary Video). The concretion has split such that a small block reveals both dorsal and ventral flaps on the anterior left of the specimen (Extended Data Fig. 2, Supplementary Video). The tripartite carapace (Extended Data Figs 3, 4, Supplementary Video) extends well in front of the head; the

largest isolated carapace element exceeds 1 m in length, indicating individuals more than 2 m in overall length. The frontal appendages are composed of seven podomeres (Fig. 2a, b, Extended Data Fig. 5a-c). The long proximal podomere bears a short, backwardly directed ventral spine with a comb-like array of spines on its posterior margin (Figs 2a, b, Extended Data Fig. 5a-c). The five succeeding short podomeres bear long, ventral spines curving forward distally (Fig. 2c, Extended Data Figs 5d-g, 6, 7). These ventral spines were canted inward at ca 45 degrees to the longitudinal axis of the appendage (Extended Data Fig. 5a-c). They carry ca 80 long, mobile, laterally flattened, flexible setae on their anterior margin. These setae bear two rows of densely spaced fine spinules set in a V on their dorsal margin (Fig. 2, Extended Data Fig 6). The terminal pointed podomere of the appendage lacks spines (Fig. 2a, b, Extended Data Fig. 5a-c). No eyes or oral cone have yet been found. In the trunk, dorsal and ventral flaps are non-overlapping and separated from each other by intervening body wall (Fig. 1, Extended Data Figs 1 and 2, Supplementary Video). Both have densely spaced transverse rods composed of short, flared, hollow cones one inserted into another; the basal cone is substantially larger than those succeeding it (Fig. 1h). The holotype YPM 237172 shows that segmentally arranged bands of thin, flexible setal blades attach at the base of the dorsal flaps and traverse the animal dorsally (Fig. 1, Extended Data Fig. 1). Individual setal blades connect to each other a short distance behind their anterior margin (Extended Data Fig. 8e). The blades have rounded terminations and show the presence of fine lamellae, probably on both sides (Fig. 1i, Extended Data Fig. 8). There is no evidence for the presence of a tail fan. A reconstruction of *A. benmoulae* is provided in Fig. 3.

The discovery of dorsal flaps in *Aegirocassis benmoulae* warranted re-examination of Cambrian anomalocaridids, given that the presence of dorsal flaps is difficult to demonstrate in flattened specimens owing to compaction and the tendency of the shale to split along one plane. Specimens of *Peytoia nathorsti* from the Burgess Shale revealed clear evidence of their presence in USNM 274161 (Extended Data Fig. 9a-c), and possibly USNM 274145 (Extended Data Fig. 9e). There are also indications of two sets of flaps in *Hurdia* (ROM 49930 and ROM 59320) but in this case the evidence is more circumstantial (see Supplementary Text).

Given their phylogenetic position immediately stemward of euarthropods[4, 5, 6] (Fig. 4; Extended Data Fig. 10; Supplementary text), the apparent absence of biramous appendages has been an anomalous aspect of anomalocaridid morphology. It was usually assumed that anomalocaridid lateral flaps were homologous to the flaps of gilled lobopodians such as *Kerygmachela kierkegaardi* and that ventral limbs were lost[13, 16]. The previously known flaps in Cambrian anomalocaridids[6, 11, 13-15, 18], however, overlap from posterior to anterior, the reverse of the arrangement in the more basal *Kerygmachela kierkegaardi*, *Pambdelurion whittingtoni* and *Opabinia regalis*[16, 20-22, 26]. This anomaly is resolved by the discovery of additional, dorsal flaps in *Aegirocassis benmoulae*, *Peytoia nathorsti*, and likely also *Hurdia victoria*: the position and morphology of the dorsal flaps indicates that they are homologous with those in gilled lobopodians. Thus, the larger ventral flaps in *A. benmoulae* and Cambrian anomalocaridids are here considered to be homologous with the lobopodous limbs of *K. kierkegaardi* and *P. whittingtoni*. This interpretation is supported by the presence of limbs in the anomalocaridid *Cucumericrus*

*decoratus*[14], which shows lobopodous walking limbs overlain dorsally by a single set of flaps (see Supplementary Text). The setal blades in *A. benmoulae* and other anomalocaridids, which are attached to the dorsal flaps and overlie the trunk, are likely homologous with the less extensive "gill-like" wrinkled structures on the flaps of *K. kierkegaardi* and *P. whittingtoni*[20, 21], and the setal blades in *O. regalis*[5, 16, 22] (Fig. 4), although an alternative interpretation for these last has been advanced[26].

It has been suggested that the Cambrian biramous limb arose through the sclerotisation of the lobopodous walking limb and its fusion with the dorsal flap of gilled lobopodians, which was reduced to leave the gill as an exite[5, 16, 23]. The presence of a dorsal gill-bearing flap inserting separately to the ventral limb-derived flap in *A. benmoulae* and other anomalocaridid taxa indicates that they pre-date the acquisition of biramous limbs. This confirms their place on the euarthropod stem (Fig. 4, Extended Data Fig. 10; Supplementary Text), resolving the debate on their phylogenetic position in line with recent neurological evidence[6].

Among arthropods, the size of *Aegirocassis benmoulae* (over 2 m in length) is paralleled only by some pterygotid eurypterids[27] and terrestrial arthropleurids[28]. The evolution of gigantic filter-feeders within clades of nektic macrophagous predators is well documented in Mesozoic pachycormid fish[29] and Cenozoic sharks and whales[30]. The huge size of *A. benmoulae* represents a much earlier example of a filter-feeding life-style correlating to gigantism. The abundance of gigantic anomalocaridid filter-feeders in the high palaeolatitude Fezouata Biota points to a complex planktic ecosystem. Early

Cambrian anomalocaridid filter feeders also fed on zooplankton, but they remained relatively small[9]. Although the Cambrian Explosion saw the establishment of the first complex planktic ecosystems, the convergent (Supplementary Text) rise of giant filter-feeding anomalocaridids during the Ordovician followed an increase in the abundance and diversity of phytoplankton and a consequent zooplankton radiation as part of the Great Ordovician Biodiversification Event[25].

**Online Content**

Methods, Extended Data display items and Source Data are available in the online version of the paper; references unique to these sections appear only in the online paper.

**References**


1. Ma, X., Hou, X, Edgecombe, G. D. & Strausfeld, N. J. Complex brains and optic lobes in an early Cambrian arthropod. *Nature* **490**, 258-261 (2012).
2. Yang, J., Ortega-Hernández, J., Butterfield, N. J. & Zhang, Z. Specialized appendages in fuxianhuiids and the head organization of early euarthropods. *Nature* **494**, 468-471 (2013).
3. Tanaka, G., Hou, X., Ma, X., Edgecombe, G. D. & Strausfeld, N. J. Chelicerate neural ground pattern in a Cambrian great appendage arthropod. *Nature* **502**, 364-367 (2013).
4. Budd, G.E. A palaeontological solution to the arthropod head problem. *Nature* **417**, 271-275 (2002).

5. Daley, A. C., Budd, G. E., Caron, J.-B., Edgecombe, G. D. & Collins, D. The Burgess Shale anomalocaridid *Hurdia* and its significance for early euarthropod evolution. *Science* **323**, 1597–1600 (2009).
6. Cong, P., Ma, X., Hou, X., Edgecombe, G. D. & Strausfeld, N. J. Brain structure resolves the segmental affinity of anomalocaridid appendages. *Nature* **513**, 538-542 (2014).
7. Daley, A. C. & Budd, G. E. New anomalocaridid appendages from the Burgess Shale, Canada. *Palaeontology* **53**, 721-738 (2010).
8. Paterson, J. R., García-Bellido, D. C., Lee, M. S. Y., Brock, G. A., Jago, J. B. & Edgecombe, G. D . Acute vision in the giant Cambrian predator *Anomalocaris* and the origin of compound eyes. *Nature* **480**, 237–240 (2011).
9. Vinther, J., Stein, M., Longrich, N. R. & Harper, D. A. T. A suspension-feeding anomalocarid from the Early Cambrian. *Nature* **507**, 496-499 (2014).
10. Daley, A. C. & Bergström, J. The oral cone of *Anomalocaris* is not a classic "peytoia". *Naturwissenschaften* **99**, 501–504 (2012).
11. Whittington, H. B. & Briggs, D. E. G. The largest Cambrian animal, *Anomalocaris*, Burgess Shale, British Columbia. *Phil. Trans . R. Soc. B.* **309**, 569-609 (1985).
12. Bergström, J. *Opabinia* and *Anomalocaris*, unique Cambrian 'arthropods'. *Lethaia* **19**, 241-246 (1986).
13. Chen, J., Ramsköld, L. & Zhou, G. Evidence for monophyly and arthropod affinity of Cambrian giant predators. *Science* **264**, 1304–1308 (1994).
14. Hou, X., Bergström, J. & Ahlberg, P. *Anomalocaris* and other large animals in the Lower Cambrian Chengjiang Fauna of southwest China. *GFF* **117**, 163–183 (1995).

15. Collins, D. The "evolution" of *Anomalocaris* and its classification in the arthropod class Dinocarida (nov) and order Radiodonta (nov). *J. Paleont.* **70**, 280–293 (1996)

16. Budd, G. E. The morphology of *Opabinia regalis* and the reconstruction of the arthropod stem-group. *Lethaia* **29**, 1-14 (1996).

17. Van Roy, P. & Briggs, D. E. G. A giant Ordovician anomalocaridid. *Nature* **473**, 510-513 (2011).

18. Daley, A. C. & Edgecombe, G. D. Morphology of *Anomalocaris canadensis* from the Burgess Shale. *J. Paleont.* **88**, 68-91 (2013).

19. Van Roy, P., Orr, P. J., Botting, J. P., Muir, L. A., Vinther, J., Lefebvre, B., el Hariri, Kh. & Briggs, D. E. G. Ordovician faunas of Burgess Shale type. *Nature* **465**, 215-218 (2010).

20. Budd, G. E. A Cambrian gilled lobopod from Greenland. *Nature* **364**, 709-711 (1993).

21. Budd, G. E. The morphology and phylogenetic significance of *Kerygmachela kierkegaardi* Budd (Buen Formation, Lower Cambrian, N Greenland). *Trans. R. Soc. Edinburgh: Earth Sci.* **89**, 249-290 (1999).

22. Budd, G. E. & Daley, A. C. The lobes and lobopods of *Opabinia regalis* from the middle Cambrian Burgess Shale. *Lethaia*, **45**, 83–95 (2012).

23. Wolff, C. & Scholtz, G. The clonal composition of biramous and uniramous arthropod limbs. *Proc. R. Soc. London B* **275**, 1023-1028 (2008).

24. Haug, J. T, Waloszek, D., Maas, A., Liu, Y. & Haug, C. Functional morphology, ontogeny and evolution of mantis shrimp-like predators in the Cambrian. *Palaeontology* **55**, 369–399 (2012).

25. Servais, T., Owen, A. W., Harper, D. A. T., Kröger, B. & Munnecke, A. The Great Ordovician Biodiversification Event (GOBE): The palaeoecological dimension. *Palaeogeogr. Palaeoclim. Palaeoecol.* **294**, 99-119 (2010).

26. Zhang, X. & Briggs, D. E. G. The nature and significance of the appendages of *Opabinia* from the Middle Cambrian Burgess Shale. *Lethaia* **40**, 161–173 (2007).

27. Braddy, S. J., Poschmann, M. and Tetlie, O. E. Giant claw reveals the largest ever arthropod. *Biol. Lett.* **4**, 106-109 (2008).

28. Schneider, J. and Werneburg, R. *Arthropleura* und Diplopoda (Arthropoda) aus dem Unter-Rotliegend (Unter-Perm, Assel) des Thüringer Waldes (Südwest-Saale-Senke). *Veröff. Naturhist. Mus. Schleusingen* **13**, 19-36 (1998).

29. Friedman, M., Shimada, K, Martin, D. L., Everhart, M. J., Liston, J., Maltese. A. & Triebold, M. 100-million-year dynasty of giant planktivorous bony fishes in the Mesozoic seas. *Science* **327**, 990-993 (2010).

30. Marx, F. G. & Uhen, M. D. Climate, critters, and cetaceans: Cenozoic drivers of the evolution of modern whales. *Science* **327**, 993-996 (2010).

**Supplementary information** is linked to the online version of the paper at www.nature.com/nature.

**Acknowledgements** Mohamed and Brahim "Ou Said" Ben Moula discovered the specimens and provided support in the field. S. Beardmore, D. Field, A. Little, R. Racicot and O.E. Tetlie assisted with fieldwork in 2011. L. Ben Moula and B. Tahiri provided practical assistance. J.-B. Caron loaned specimens of *Hurdia* from ROM collections. S.

Butts and J. Utrup, K. Hollis and D. Erwin curated specimens and facilitated access to the collections at the YPM and USNM respectively. N. Utrup built custom cradles to support the articulated specimens. J. Vinther and P. Hull discussed filter-feeding and gigantism, and J. Lamsdell eurypterid book gills and phylogenetic methodology. E. Martin made available precise biostratigraphical data for the localities. G. Edgecombe provided unpublished observations on *Cucumericrus*. M. Collins discussed appendage function and prepared the digital reconstruction. M. Fox advised on preparation and consolidation techniques and provided equipment. C. Graham and J. Slawski provided support and access to digital imaging facilities. The initial part of the research was carried out while PVR was at Ghent University and in receipt of a mobility grant from the Biology Commission of the Research Foundation – Flanders (FWO). ACD was financially supported by the Swedish Research Council (Vetenskapsrådet) and the Oxford University Museum of Natural History. The research was supported by NSF Grant EAR-1053247 and by the Division of Invertebrate Paleontology, Yale Peabody Museum of Natural History.

**Author Contributions** All authors, led by PVR, participated in the interpretation of the material and reconstruction of *A. benmoulae* and contributed to the writing and editing of the manuscript. PVR and ACD examined the material of *P. nathorsti* at the USNM and conducted the phylogenetic analyses. PVR conducted fieldwork in Morocco, prepared and photographed Fezouata specimens, made preliminary reconstructions, and composed the figures. ACD photographed Burgess Shale specimens, prepared all explanatory specimen drawings and made the Burgess Shale figure.

**Author information** Reprints and permissions information is available at www.nature.com/reprints. The authors declare no competing financial interests. Correspondence and requests for materials should be addressed to PVR (peter.vanroy@yale.edu).

**Text Figure captions**

**Figure 1 | *A. benmoulae,* holotype YPM 237172, Early Ordovician, Fezouata Biota, Morocco. a-d**, dorsal view: **a**, part, showing ventral flaps. **b**, part, separate block in place, showing dorsal flaps. **c**, interpretative drawing combining part and counterpart. **d**, part, matrix surrounding dorsal flaps digitally removed to show both sets of flaps. **e-g**, lateral view: **e**, part; **f**, part, dorsal flaps added from counterpart. **g**, interpretative drawing combining part and counterpart. **h**, part, transverse rods composed of hollow cones of third ventral flap. **i**, counterpart, oblique view of anterior free end of setal blades showing lamellae laterally. Arabic numerals indicate trunk somites.

**Figure 2 | *A. benmoulae,* appendages and ventral spines, Early Ordovician, Fezouata Biota, Morocco. a**, complete frontal appendage with partial ventral spines, showing mobile spinulose filtrating setae, paratype YPM 527125. Detail of the spinulose filtrating setae is provided in Extended Data Fig. 6a. **b**, interpretative drawing of YPM

527125. **c**, partial appendage with complete ventral spines, paratype YPM 222227. Roman numerals indicate appendage podomeres.

**Figure 3 | *A. benmoulae,* reconstruction, Early Ordovician, Fezouata Biota, Morocco.** Eye shape and position inferred from related taxa, with position further supported by the posterior gape between the carapace elements. The eyes are deliberately depicted comparatively smaller than in other anomalocaridids: to achieve visual acuity comparable to that of more diminutive forms, a large animal requires smaller eyes relative to its body size. In addition, a filter-feeding life-style demands less acute vision than a macropredatory mode of life, further reducing the need for large eyes. Reconstruction by M. Collins.

**Figure 4 |** Simplified cladogram showing the position of *Aegirocassis benmoulae*, and schematic cross-sections through the bodies of included taxa illustrating the limb homologies and morphological transitions. The position of setal blades in *Cucumericrus decoratus* is uncertain. A more extensive cladogram is provided in Extended Data Fig. 10.

**Methods**

The Fezouata specimens are housed in the collections of the Yale Peabody Museum of Natural History (YPM), while the *Peytoia* material examined is at the National Museum

of Natural History (USNM) and the *Hurdia* fossils used for this paper are in the collections of the Royal Ontario Museum (ROM).

The Moroccan specimens were mechanically prepared using PaleoTools ME9100, PaleoAro, MicroJack5 and MicroJack1 air scribes, and needles and scalpels. Specimens were glued with Paraloid B-72 dissolved in acetone, after which they received a protective coat of consolidant, consisting of a 5 percent solution of Butvar B-98 in ethanol.

For photography, the Moroccan specimens were illuminated by a 500 W tungsten floodlight with an Aflash Photonics linear polariser in front; a Cokin XPro X164 circular polariser was mounted on the camera lens and crossed with the polariser of the light source to maximise contrast. All parts were lit from the north-west. With the exception of the flaps, counterparts were illuminated from the south-west and mirrored in Adobe Photoshop CC 2014 to create a false positive relief image and facilitate direct comparison of part and counterpart. In some cases, where indicated, information from part and counterpart was combined digitally into a single image in Adobe Photoshop CC 2014 to facilitate interpretation. All specimens were photographed dry, with the exception of YPM 227934, which was imaged under ethanol.

The micrograph of the muscle tissue in Extended Data Fig. 2g was taken with a Leica DFC 425 digital camera attached to a Leica MZ16 binocular microscope with a Leica Plan APO 1X lens and steered from a computer through Leica Application Suite 4.2. All

other photographs were taken with a Hasselblad H4D-200MS medium frame digital SLR attached to a computer and operated remotely in 6-shot mode through Hasselblad Phocus 8.2.1 software to acquire images of 200 MP resolution. Overview photographs of YPM 237172 employed a Hasselblad HC 2.8/80 mm lens stopped down to f/8; close-ups and all other, smaller specimens were photographed with a Hasselblad HC Macro 4/120 mm II lens stopped down to f/9.5. Lens distortion was corrected using Hasselblad Phocus 8.2.1 software. Stacks of between 10 and 50 images were taken in aperture priority mode, with manual focussing through the focal plane. After exporting the FFF format digital negatives to TIFF from Hasselblad Phocus 8.2.1, the photographs were stacked in Zerene Stacker 1.04 (64 bit) using the PMax pyramid stack algorithm. The stacked images were then post-processed in Adobe Photoshop CC 2014, first applying the "Sharpen more" and "Sharpen" functions, followed by removal of the background. Levels were then manually balanced while holding down the "alt" key to prevent clipping of pixels in the specimen; the grey level was always retained at 50 percent. In a few cases, some minor adjustments were made to the exposure. The high-resolution images were down-sampled in Adobe Photoshop CC 2014 to lower resolution TIFF files for use in the plates.

The Burgess Shale specimens were imaged immersed in water, with polarised lighting sourced from the north-west; a second polariser in front of the camera lens was crossed with the polarisation of the light source to enhance contrast. Photographs were taken using a Canon EOS500D small frame digital SLR controlled remotely using the EOS Utility 2.8.1.0 program. The camera was fitted with a Canon EF-S 60 mm Macro Lens, which was stopped down to F/2.8 (Extended Data Fig. 9d), F/3.5 (Extended Data Fig.

X9a), F/4.0 (Extended Data Fig. 9b) or F/4.5 (Extended Data Fig. 9e). Images were post-processed in Adobe Photoshop CS6 using the "Sharpen" function, minor adjustments were made to the exposure, and the background was removed were necessary. Extended Data Figure 9 was created using Adobe Illustrator CS6.

Explanatory drawings of the specimens were prepared in Adobe Illustrator CS6 based on the high-resolution images. Photographs of part and counterpart with used to create composite drawings. The drawings are consistently colour-coded to allow identification of anatomical structures.

**Extended Data Figure captions**

**Extended Data Figure 1 | *A. benmoulae*, nearly complete three-dimensionally preserved specimen, counterpart, dorsal view, Early Ordovician, Fezouata Biota, Morocco, holotype YPM 237172. a**, with separate blocks in place, showing ventral flaps. **b**, with one block removed, showing dorsal flaps. **c**, with two blocks removed, showing dorsal flaps alone. **d**, digital combination of images, showing both dorsal and ventral flaps. **e**, interpretative drawing of dorsal view combining information from part and counterpart. Arabic numerals indicate trunk somites.

**Extended Data Figure 2 | *A. benmoulae*, nearly complete three-dimensionally preserved specimen, dorsal and ventral flaps, Early Ordovician, Fezouata Biota, Morocco, holotype YPM 237172. a**, separate block, part, dorsal flaps, plan view. **b**,

separate block, lateral view showing body wall (counterpart), and dorsal (part) and ventral flaps (counterpart). **c**, separate block, counterpart, ventral flaps. **d**, counterpart, dorsal flaps. **e**, interpretative drawing of lateral view of separate block. **f**, part, ventral flaps. **g**, part, muscle tissue closely associated with first dorsal flap on left side, showing individual fibres.

**Extended Data Figure 3 | *A. benmoulae,* central elements of carapace, Early Ordovician, Fezouata Biota, Morocco. a**, **b**, YPM 516785: **a**, nearly complete central element, part, dorsal view. **b**, interpretative drawing. **c**, **d**, paratype YPM 227556: **c**, nearly complete element, part, dorsal view,. **d**, interpretative drawing. **e**, **f**, YPM 523425: **e**, ventral triangular extension, counterpart, showing marginal rim and texture. **f**, interpretative drawing. **g, h**, YPM 523424: **g**, partial central element, part, oblique, showing second morph with additional anterior triangular extension. **h**, interpretative drawing.

**Extended Data Figure 4 | *A. benmoulae*, complete carapace lateral element associated with partial central element, Early Ordovician, Fezouata Biota, Morocco, paratype YPM 525437. a**, with partial central element, part, in place. **b**, with partial central element, part, removed, revealing counterpart imprint of triangular ventral extension. **c**, with dorsal side of central element digitally removed, revealing triangular ventral extension overlying anterior of lateral element. **d**, interpretative drawing.

**Extended Data Figure 5 | *A. benmoulae*, appendages and ventral spines, Early Ordovician, Fezouata Biota, Morocco. a-c**, paratype YPM 527123, nearly complete appendage: **a**, part. **b**, interpretative drawing combining part and counterpart. **c**, counterpart. **d**, YPM 527124, part, distal portion of ventral spines. Setae showing double row of spinules arrowed. YPM 527123 and 527124 belong to a disarticulated assemblage which may represent a single individual. **e**, YPM 523810, part, distal portion of five ventral spines. **f**, YPM 523428, part, termination of ventral spine. **g,** YPM 523423 and 523424, counterpart, ventral spines and partial carapace element. Roman numerals indicate appendage podomeres.

**Extended Data Figure 6 | *A. benmoulae*, appendages and appendage ventral spines, Early Ordovician, Fezouata Biota, Morocco. a**, close-up of ventral spines of YPM 527125, showing spinulose filtrating setae and their insertion on the anterior margin of the ventral spines. Setae showing double row of spinules arrowed. **b-d**, YPM 525217, partial appendage: **b**, part. **c**, interpretative drawing combining information from part and counterpart. **d**, counterpart. Roman numerals indicate appendage podomeres.

**Extended Data Figure 7 | *A. benmoulae*, Early Ordovician, Fezouata Biota, Morocco. a-c**, partial appendage, paratype YPM 222227**. a**, part. **b**, interpretative drawing combining information from part and counterpart. **c**, counterpart. Roman numerals indicate appendage podomeres. **d**, **e**, assemblage of carapace elements, appendage ventral spines and setal blades, YPM 523523-523527. **d**, specimen. **e**, interpretative drawing.

**Extended Data Figure 8 | *A. benmoulae*, isolated bands of setal blades, Early Ordovician, Fezouata Biota, Morocco. a-c**, YPM 516791: **a**, part. **b**, counterpart. **c**, close-up of counterpart, showing fine lateral lamellae on setal blades in plan view. **d**, specimen associated with YPM 527123, part, showing lamellae on setal blades. **e,**YPM 227934, part, showing connection between setal blades and division into short anterior and long posterior free parts. **f**, YPM 516792, part.

**Extended Data Figure 9 | *P. nathorsti*, articulated specimens showing dorsal flaps, middle Cambrian, Burgess Shale, Canada. a**, USNM 274156 and 274161 joined into complete specimen. White box indicates area of close-ups of USNM 274161 in **b** and **c. b, c,** USNM 274161: **b,** posterior, counterpart, showing two sets of flaps. **c**, interpretative drawing; **d,** USNM 274154, the opposite half of the split corresponding to USNM 274156 and 274161 **e,** USNM 274145. Blue arrows indicate ventral flaps, and orange arrows indicate dorsal flaps.

**Extended Data Figure 10 | Results of the phylogenetic analysis.** Strict consensus of 70 MPTs obtained under equal weighting (CI = 0.61068702; RI = 0.79761905). Numbers above nodes indicate Bremer support / standard bootstrap (1000 replicates) values; number below nodes is the jackknife (1000 replicates, P = 36) value. An identical strict consensus tree is obtained with implied weighting for all *k*-values from 3 to 8.

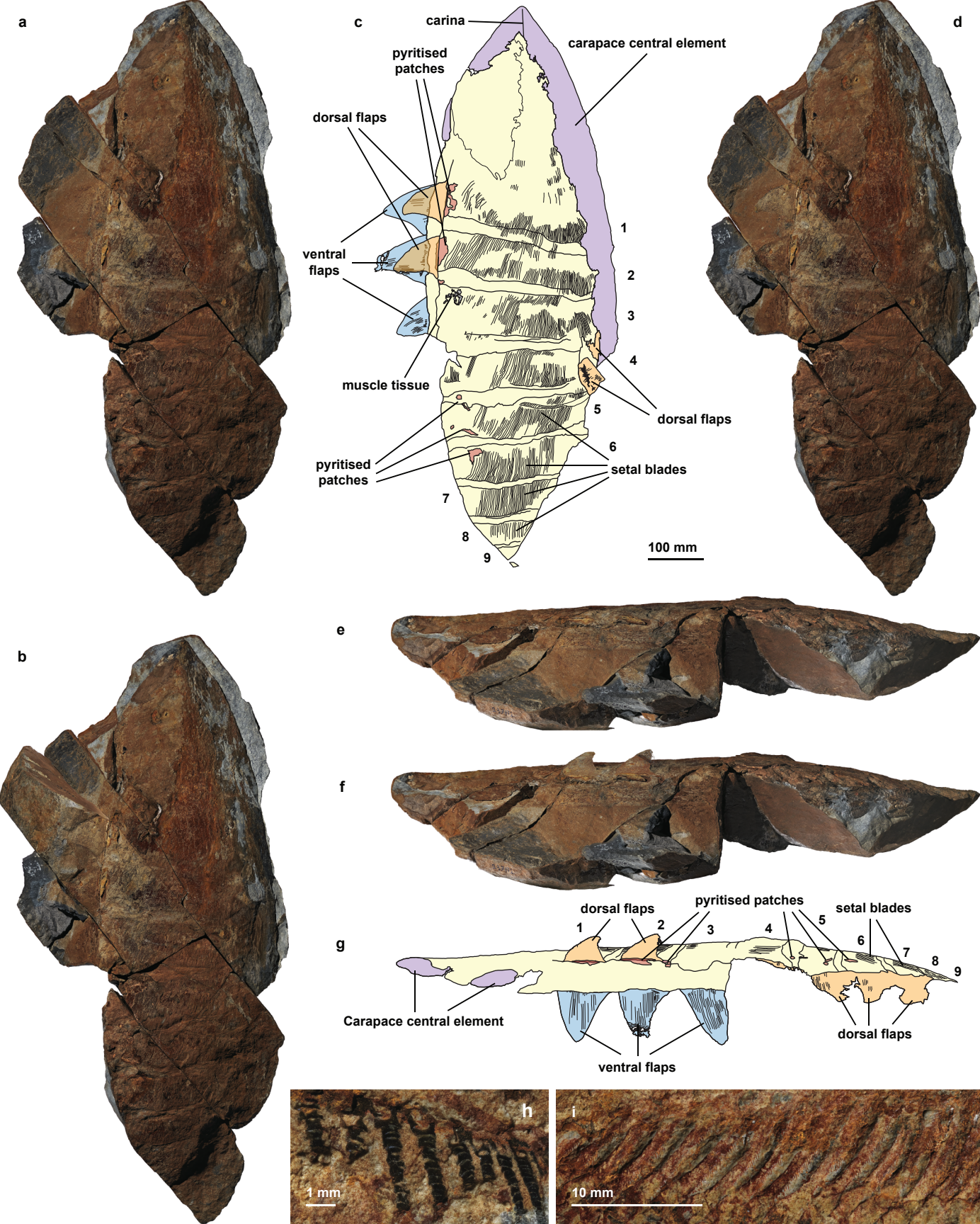
a
b
c
carina
carapace central element
pyritised patches
dorsal flaps
ventral flaps
muscle tissue
dorsal flaps
pyritised patches
setal blades
1
2
3
4
5
6
7
8
9
100 mm
d
e
f
g
dorsal flaps
pyritised patches
setal blades
Carapace central element
dorsal flaps
ventral flaps
h
1 mm
i
10 mm

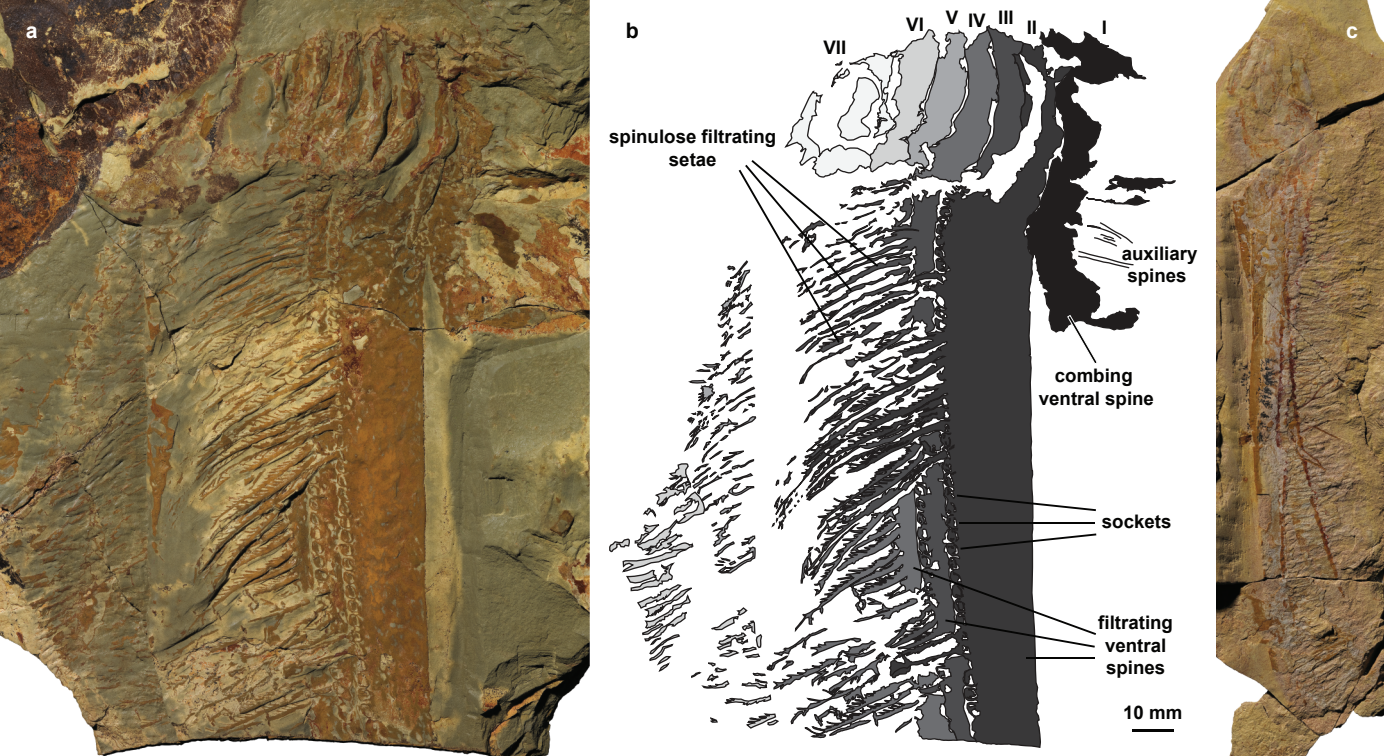
a
b
c
VII
VI
V
IV
III
II
I
spinulose filtrating setae
auxiliary spines
combing ventral spine
sockets
filtrating ventral spines
10 mm

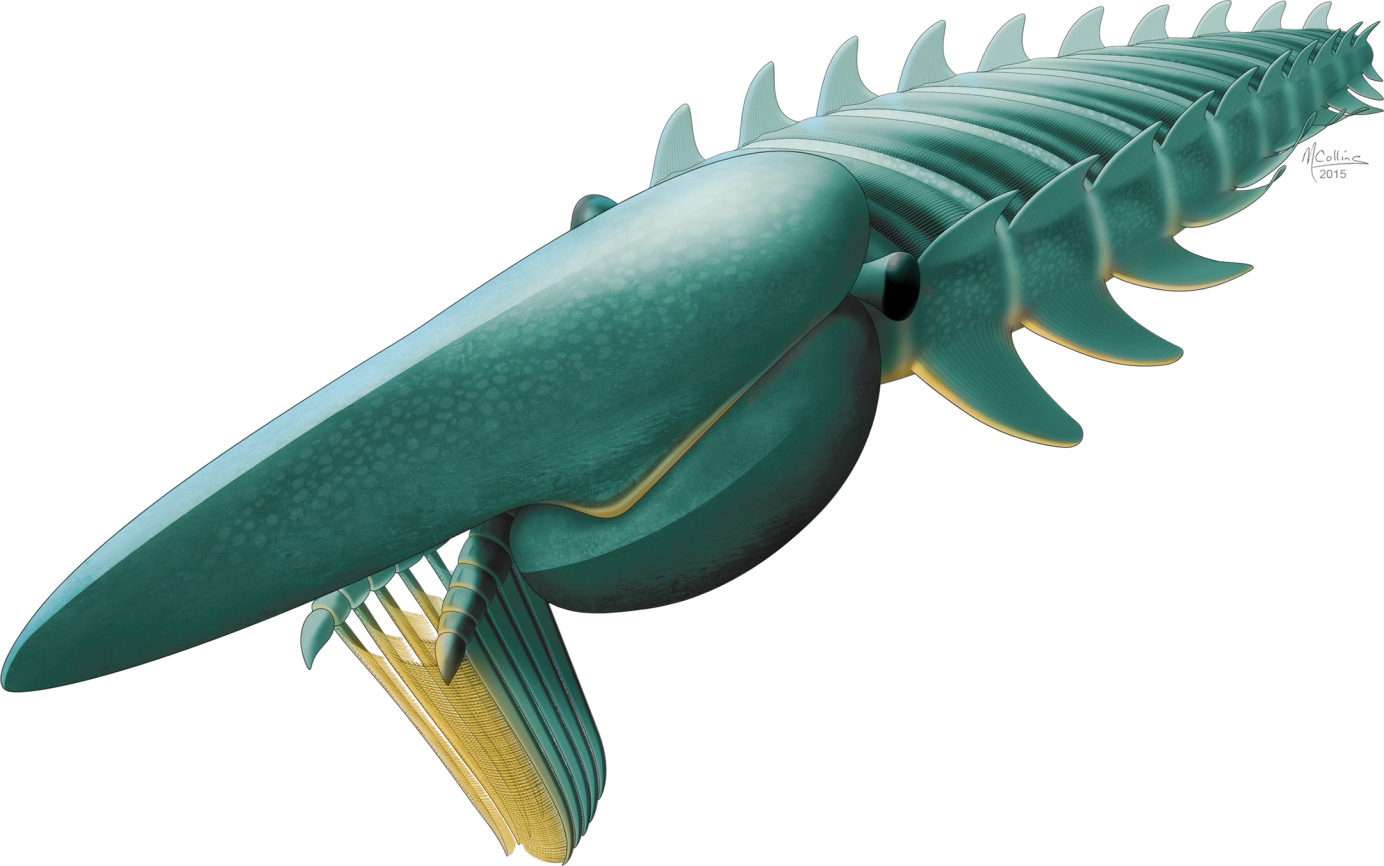
MCollins
2015

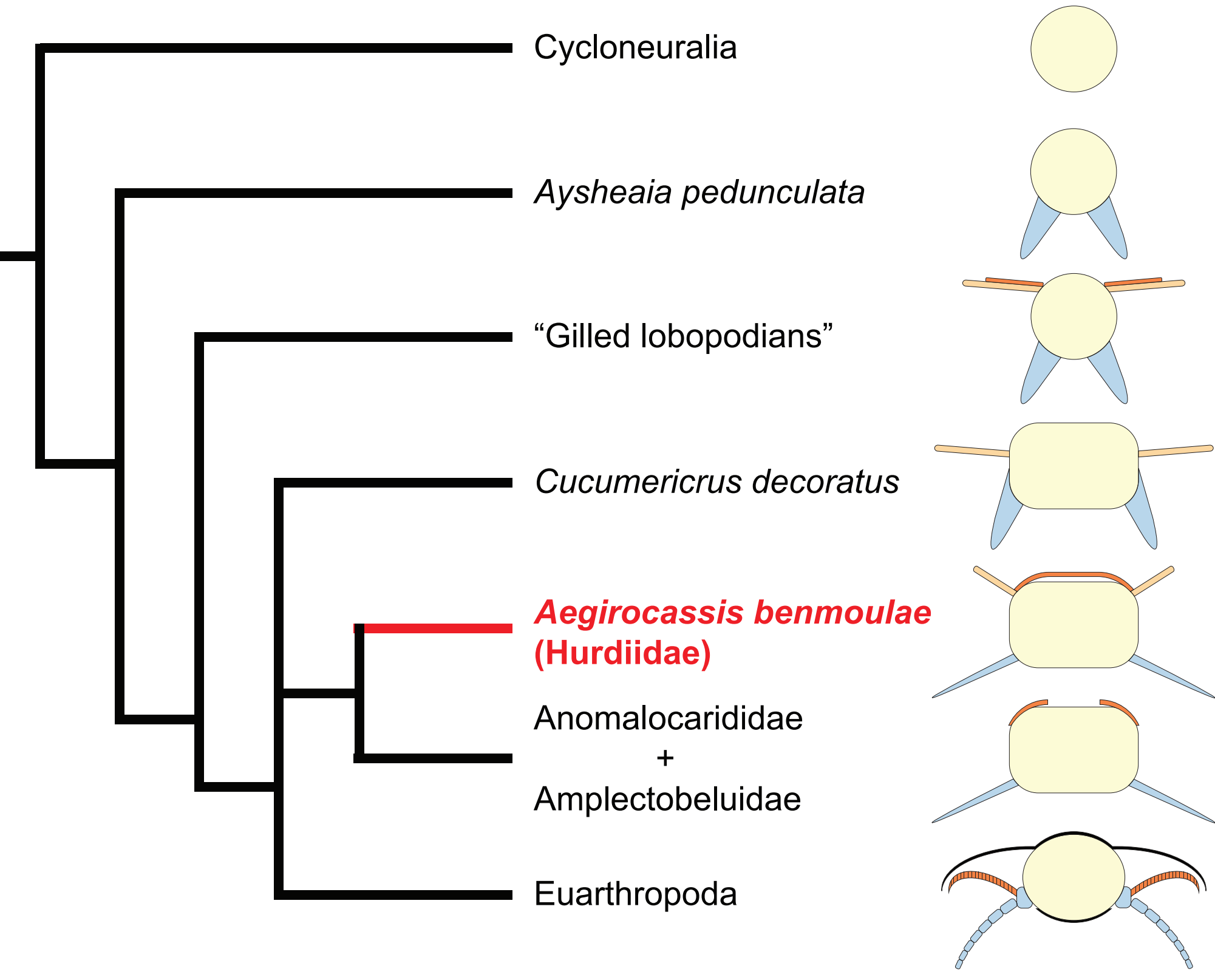
Cycloneuralia
*Aysheaia pedunculata*
“Gilled lobopodians”
*Cucumericrus decoratus*
***Aegirocassis benmoulae***
**(Hurdiidae)**
Anomalocarididae
+
Amplectobeluidae
Euarthropoda

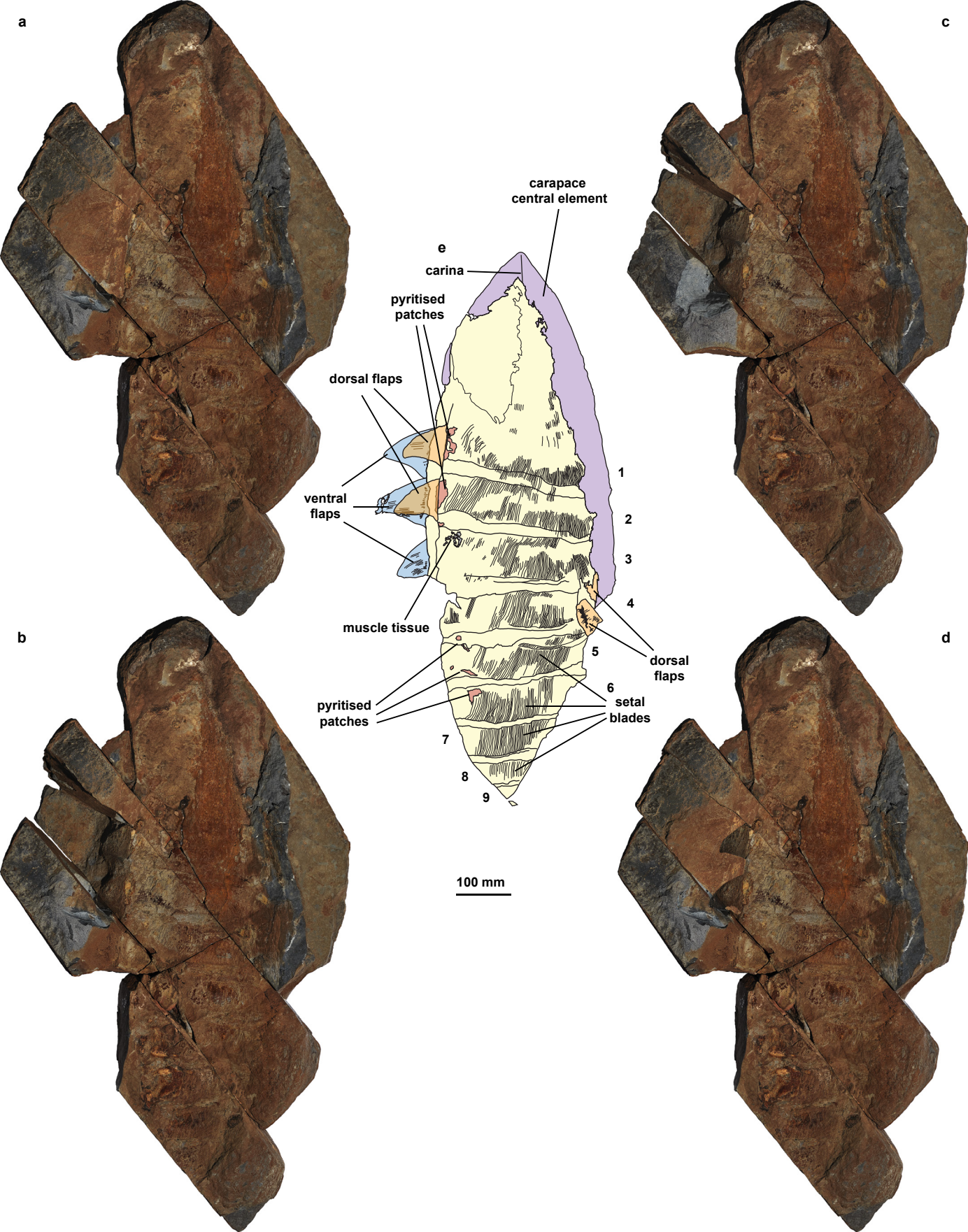
a
b
c
d
e
carapace
central element
carina
pyritised
patches
dorsal flaps
ventral
flaps
muscle tissue
dorsal
flaps
setal
blades
pyritised
patches
1
2
3
4
5
6
7
8
9
100 mm


a


b

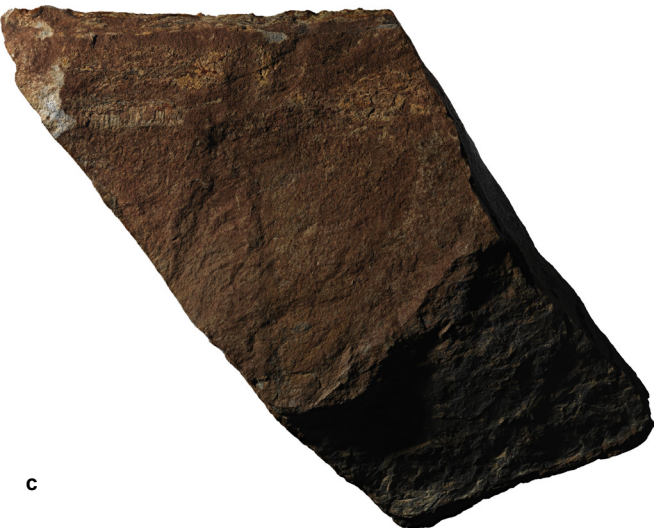
c


d

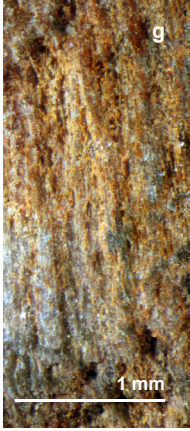
g
1 mm

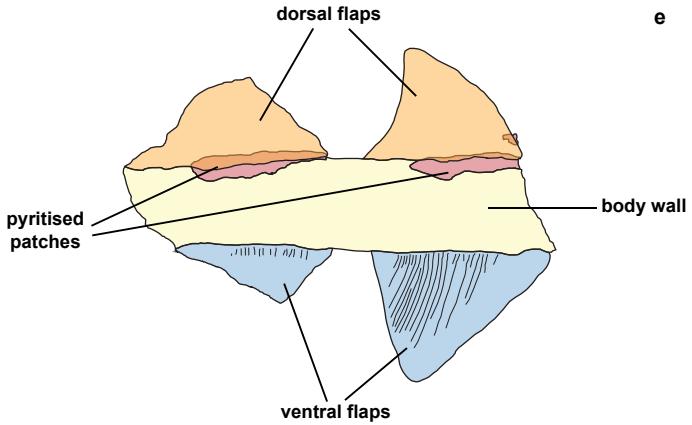
e
dorsal flaps
pyritised patches
body wall
ventral flaps

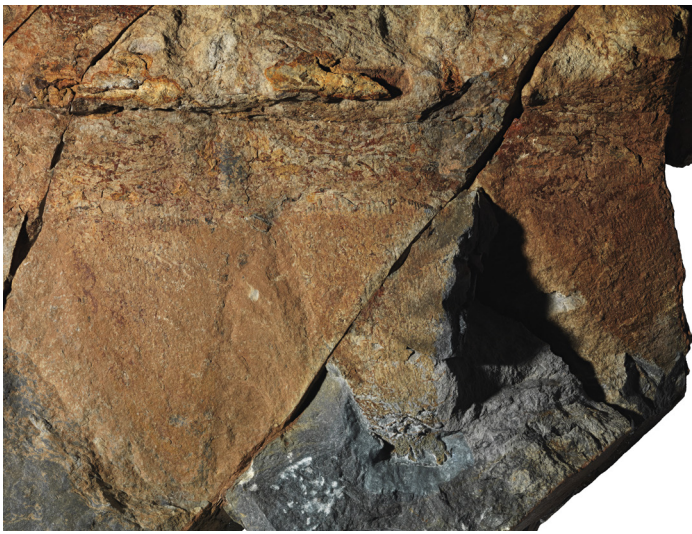
100 mm
f

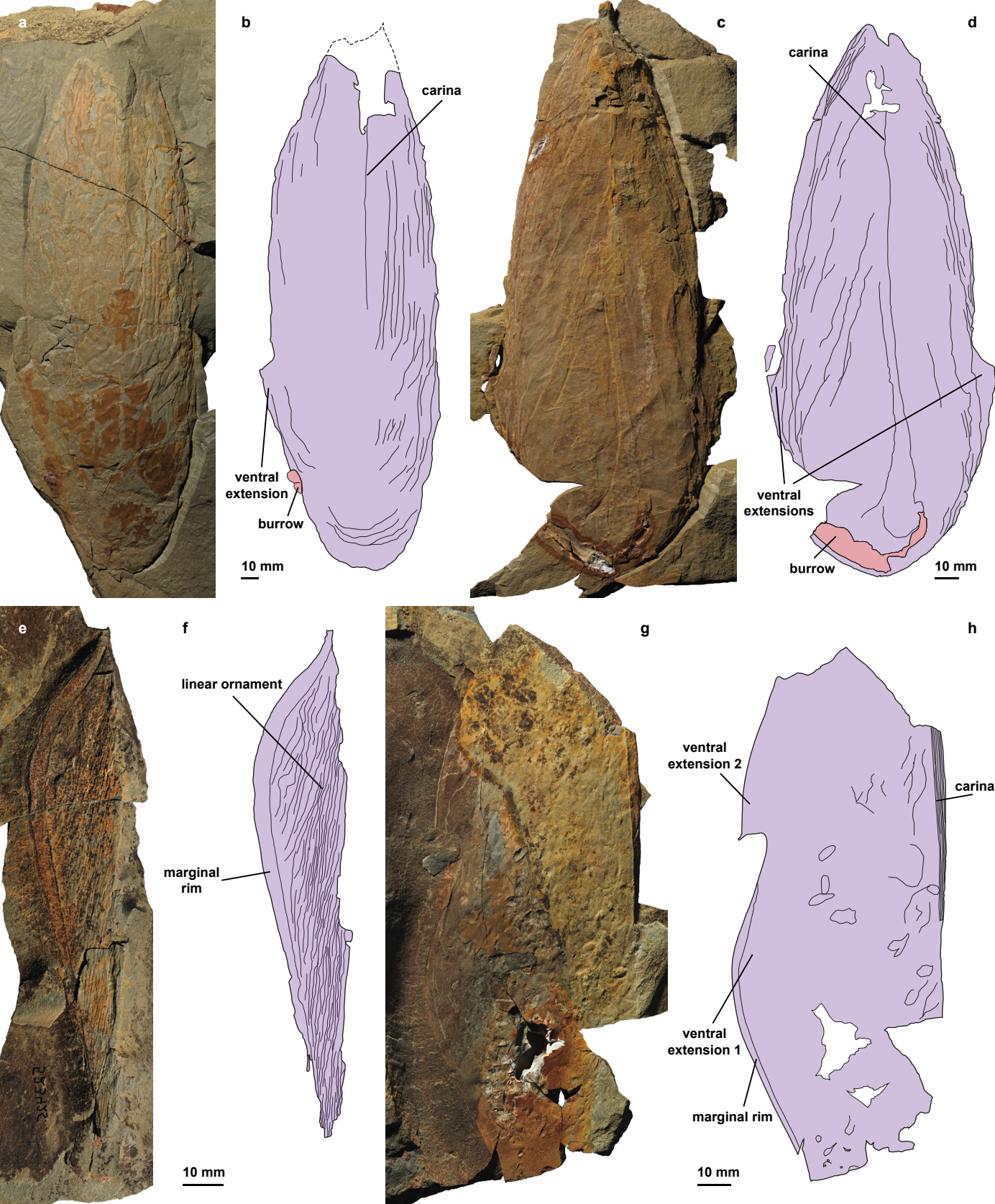
a
b
carina
ventral
extension
burrow
10 mm
c
d
carina
ventral
extensions
burrow
10 mm
e
f
linear ornament
marginal
rim
10 mm
g
h
ventral
extension 2
carina
ventral
extension 1
marginal rim
10 mm

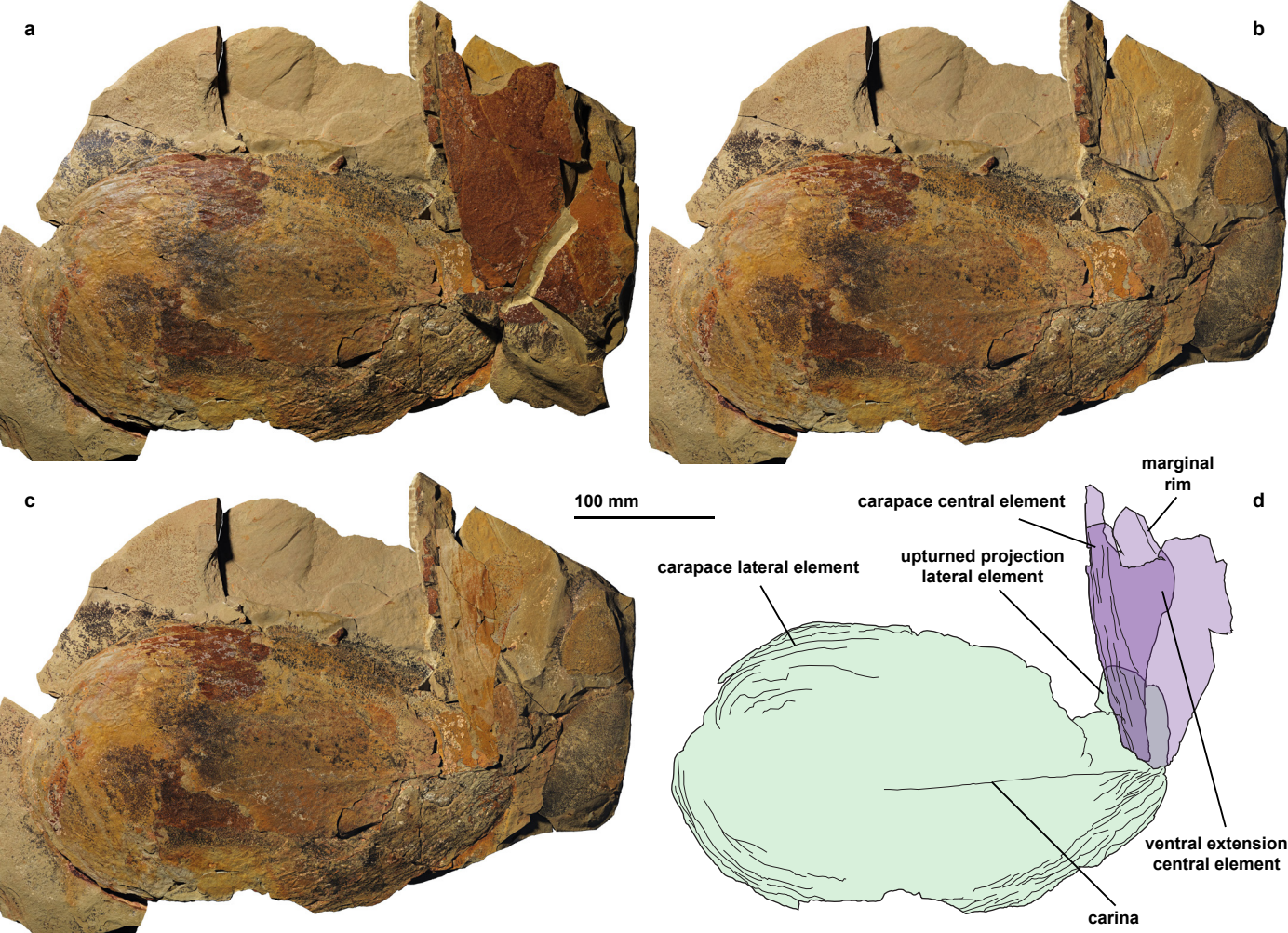
a
b
c
100 mm
d
marginal rim
carapace central element
upturned projection lateral element
carapace lateral element
ventral extension central element
carina

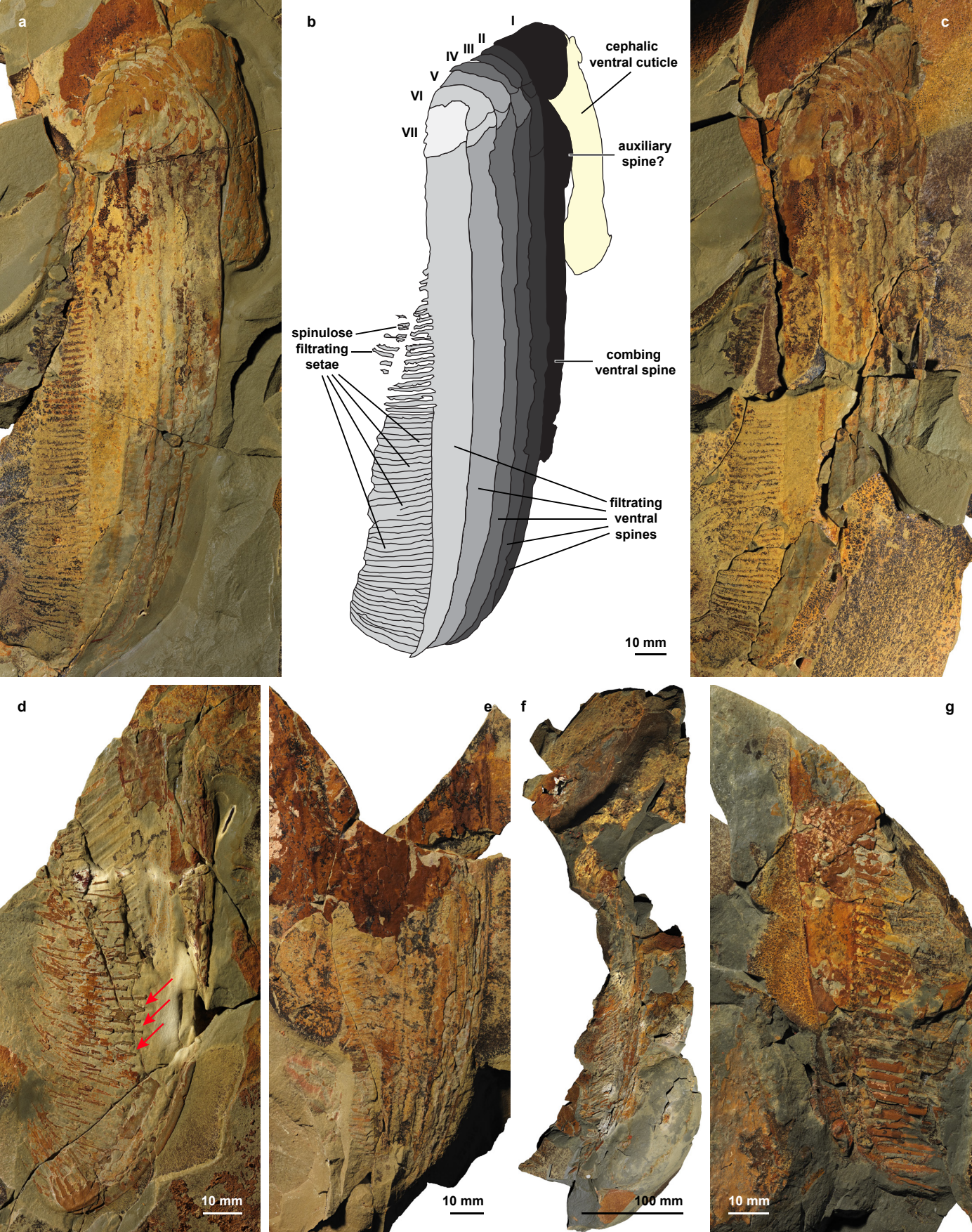
a
b
c
I
II
III
IV
V
VI
VII
cephalic ventral cuticle
auxiliary spine?
spinulose filtrating setae
combing ventral spine
filtrating ventral spines
10 mm
d
e
f
g
10 mm
10 mm
100 mm
10 mm

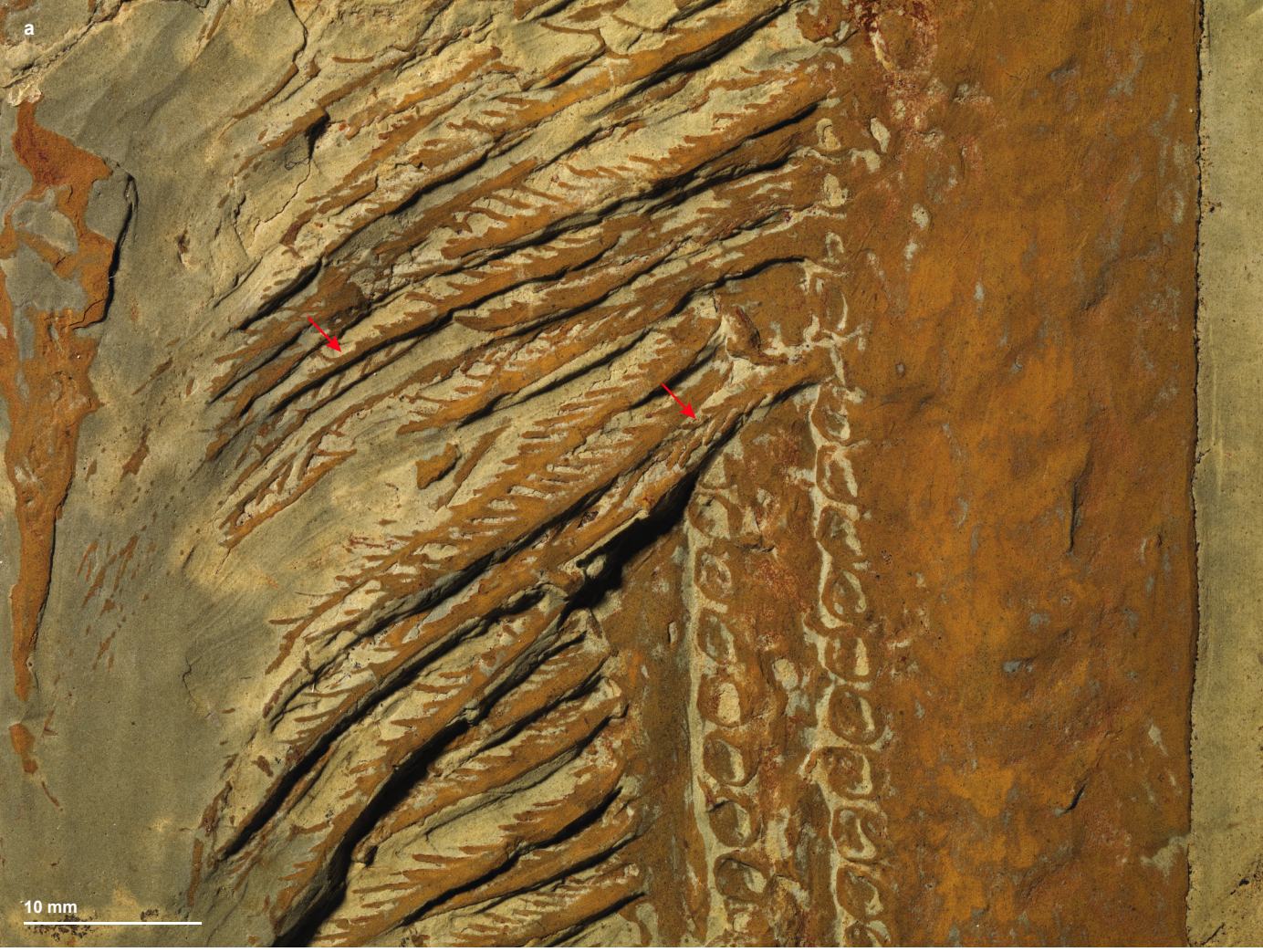
a
10 mm

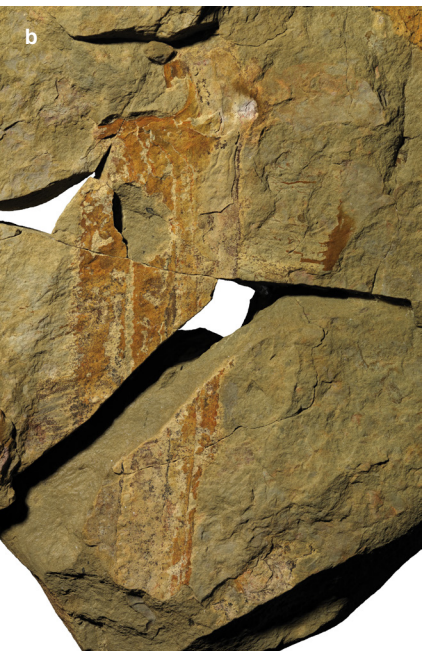
b

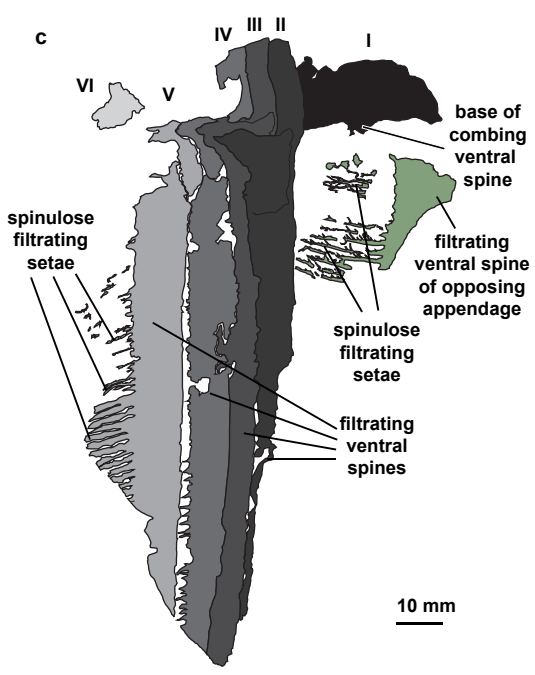
c
IV
III
II
I
VI
V
base of combing ventral spine
spinulose filtrating setae
filtrating ventral spine of opposing appendage
spinulose filtrating setae
filtrating ventral spines
10 mm


d

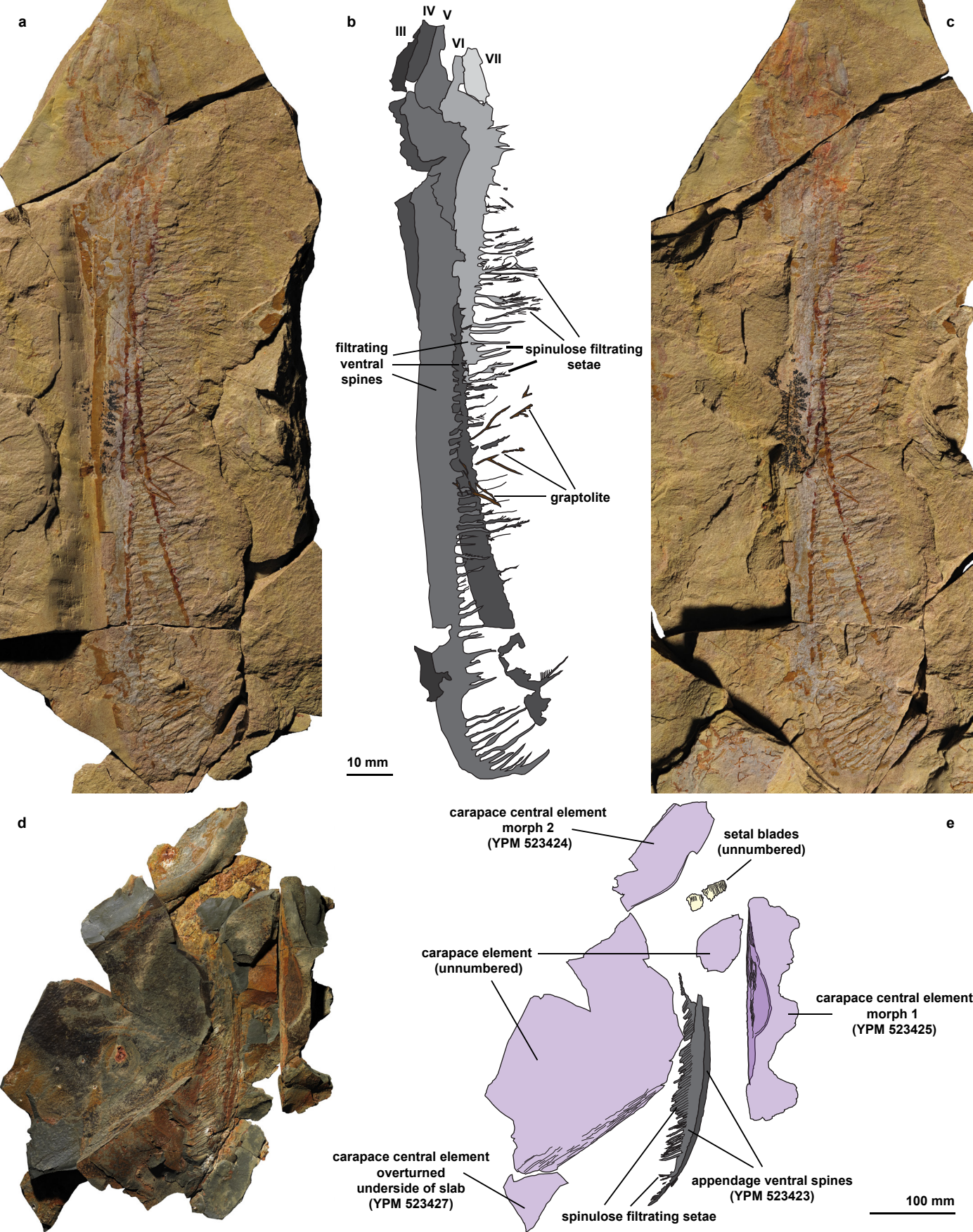
a
b
c
d
e
III
IV
V
VI
VII
filtrating ventral spines
spinulose filtrating setae
graptolite
10 mm
carapace central element morph 2 (YPM 523424)
setal blades (unnumbered)
carapace element (unnumbered)
carapace central element morph 1 (YPM 523425)
carapace central element overturned underside of slab (YPM 523427)
appendage ventral spines (YPM 523423)
spinulose filtrating setae
100 mm

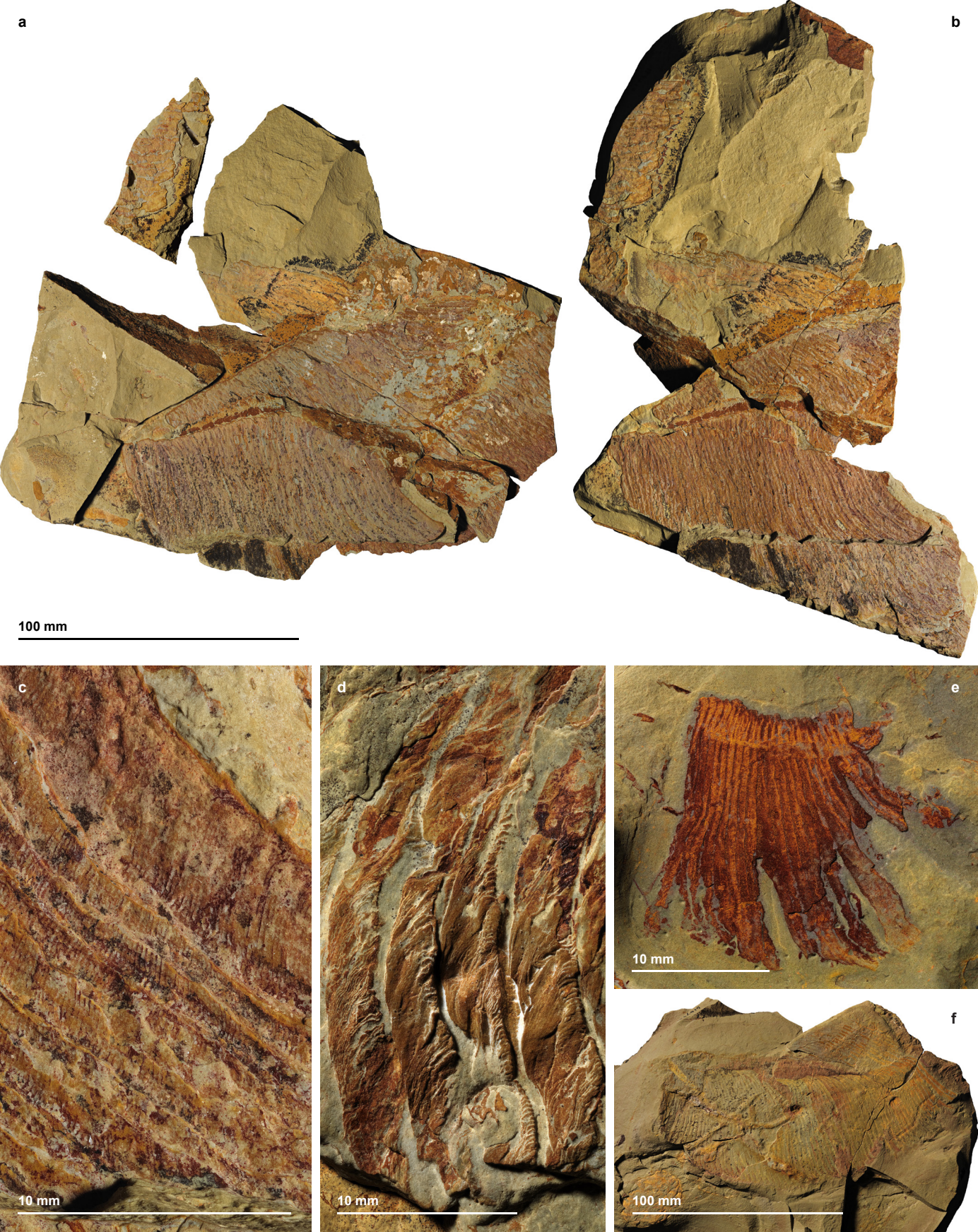
a
b
100 mm
c
10 mm
d
10 mm
e
10 mm
f
100 mm

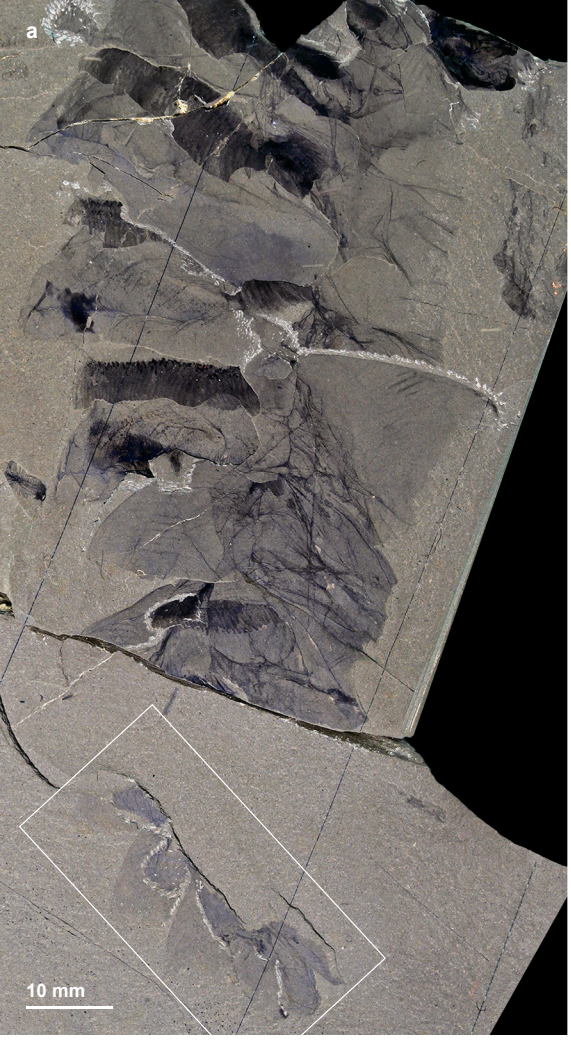
a
10 mm


b
10 mm

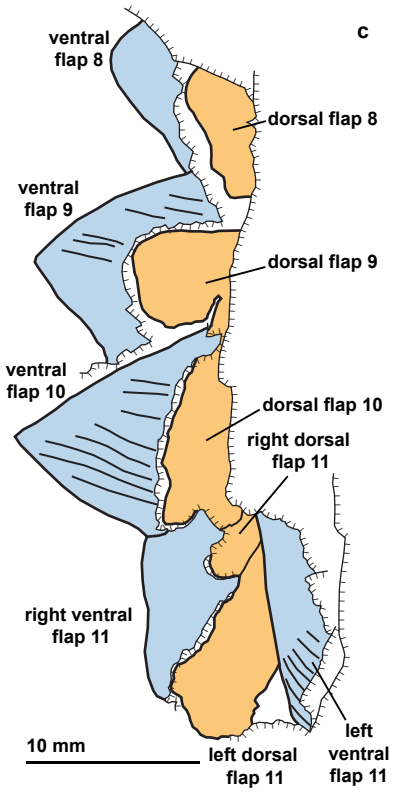
c
ventral flap 8
dorsal flap 8
ventral flap 9
dorsal flap 9
ventral flap 10
dorsal flap 10
right dorsal flap 11
right ventral flap 11
left ventral flap 11
left dorsal flap 11
10 mm

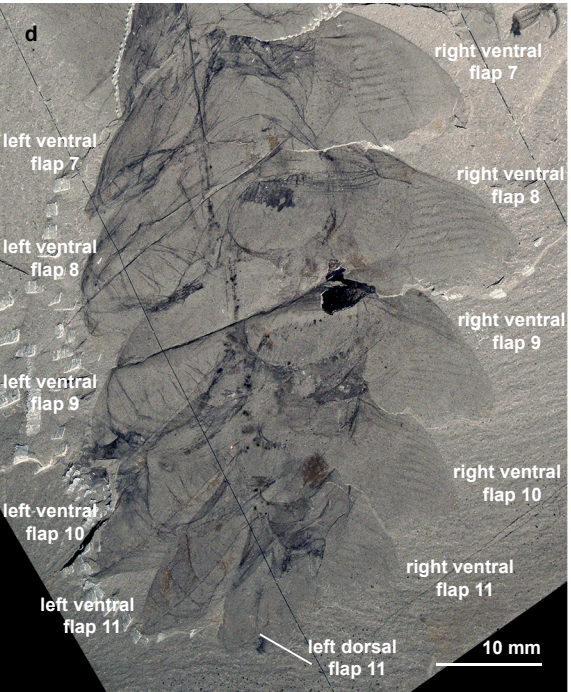
d
right ventral flap 7
left ventral flap 7
right ventral flap 8
left ventral flap 8
right ventral flap 9
left ventral flap 9
right ventral flap 10
left ventral flap 10
right ventral flap 11
left ventral flap 11
left dorsal flap 11
10 mm

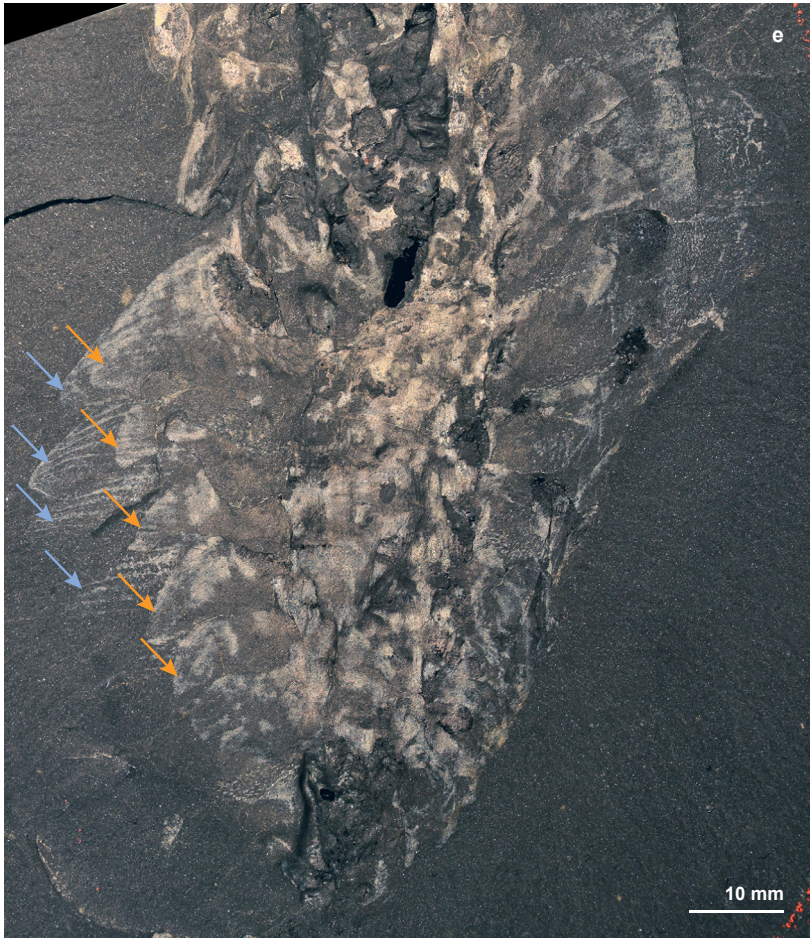
e
10 mm

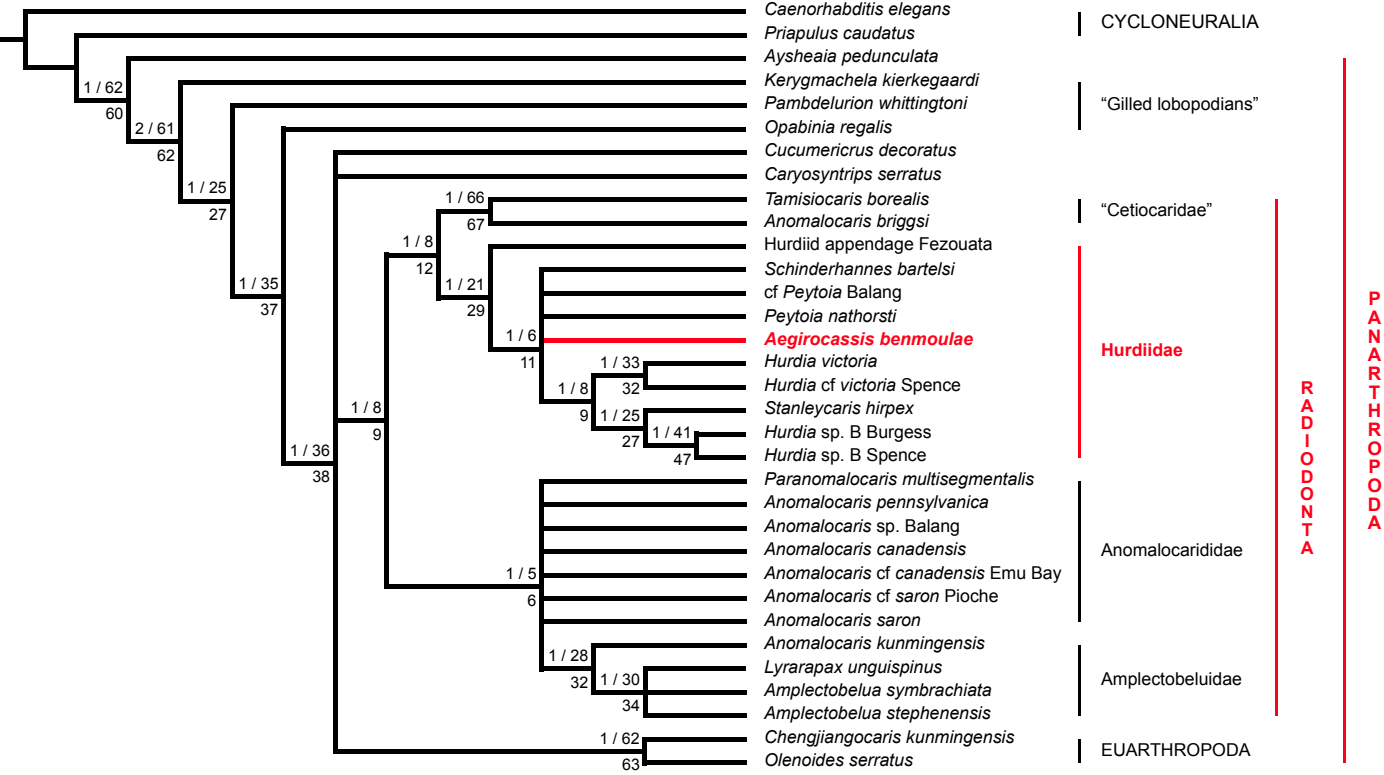
Caenorhabditis elegans
Priapulus caudatus
Aysheaia pedunculata
Kerygmachela kierkegaardi
Pambdelurion whittingtoni
Opabinia regalis
Cucumericrus decoratus
Caryosyntrips serratus
Tamisiocaris borealis
Anomalocaris briggsi
Hurdiid appendage Fezouata
Schinderhannes bartelsi
cf Peytoia Balang
Peytoia nathorsti
Aegirocassis benmoulae
Hurdia victoria
Hurdia cf victoria Spence
Stanleycaris hirpex
Hurdia sp. B Burgess
Hurdia sp. B Spence
Paranomalocaris multisegmentalis
Anomalocaris pennsylvanica
Anomalocaris sp. Balang
Anomalocaris canadensis
Anomalocaris cf canadensis Emu Bay
Anomalocaris cf saron Pioche
Anomalocaris saron
Anomalocaris kunmingensis
Lyrarapax unguispinus
Amplectobelua symbrachiata
Amplectobelua stephenensis
Chengjiangocaris kunmingensis
Olenoides serratus
1 / 62
60
2 / 61
62
1 / 25
27
1 / 35
37
1 / 36
38
1 / 8
9
1 / 66
67
1 / 8
12
1 / 21
29
1 / 6
11
1 / 33
32
1 / 8
9
1 / 25
27
1 / 41
47
1 / 5
6
1 / 28
32
1 / 30
34
1 / 62
63
CYCLONEURALIA
“Gilled lobopodians”
“Cetiocaridae”
Hurdiidae
Anomalocarididae
Amplectobeluidae
EUARTHROPODA
RADIODONTA
PANARTHROPODA